

Image Cover Sheet

CLASSIFICATION

UNCLASSIFIED

SYSTEM NUMBER

513113



TITLE

Measurements of Underwater Sound Intensity Vector

System Number:

Patron Number:

Requester:

Notes:

DSIS Use only:

Deliver to:



MEASUREMENTS OF UNDERWATER SOUND INTENSITY VECTOR

Daniel L. Hutt, Paul C. Hines and
Andrew A. J. Hamilton

Defence Research Establishment Atlantic,
P.O. Box 1012, Dartmouth, NS, Canada, B2Y 3Z7
e-mail: daniel.hutt@drea.dnd.ca

1. Abstract

Localization of underwater sound sources and characterization of ambient noise fields can be achieved through measurement of the sound intensity vector. To evaluate this concept, a passive hydrophone array called SIRA (Sound Intensity Receiver Array) has been developed for measurement of underwater sound intensity in the frequency range 100 to 6000 Hz. The array is composed of three pairs of omnidirectional hydrophones with the pairs aligned along orthogonal axes. The intensity is the time average of the product of instantaneous acoustic pressure and particle velocity. The instantaneous pressure is the average of the pressures measured by a hydrophone pair and the velocity is derived from the pressure gradient. Each hydrophone pair provides one of the components of the three dimensional intensity vector. Preliminary intensity measurements made at the Defence Research Establishment Atlantic (DREA) calibration barge facility are presented. The high angular resolution of the intensity measurements is demonstrated as well as the effect of ambient noise on the magnitude of the intensity.

2. Introduction

The sound intensity vector \hat{I} represents the magnitude and direction of the active or propagating part of an acoustic field. \hat{I} is the time averaged product of the instantaneous acoustic pressure $p(t)$ and the particle velocity vector $\hat{u}(t)$. The particle velocity is proportional to the pressure gradient which is given by the difference of signals from a pair of hydrophones. To accurately measure the gradient, the distance d between the hydrophones must be a small fraction of the wavelength, λ . Sufficiently accurate approximations to the pressure gradient can be obtained for $d < \lambda/3$. This corresponds to the condition $kd < 2$ where k is the wave number, $2\pi/\lambda$. Since the intensity measurement is based on a measurement of the pressure gradient, intensity arrays are much smaller than arrays used for conventional beamforming.

Another advantage of intensity arrays is that the difference operation which provides the gradient reduces the impact of coherent ambient noise. Since ambient noise in the ocean may have a high degree of coherence¹, intensity arrays can be well suited for underwater signal detection. For example, Lo and Junger² showed that time averaged measurements of intensity can discriminate against ambient noise even when the noise spectrum and direction of incidence coincides with that of the signal. However, the intensity array remains susceptible to the incoherent component of ambient noise and to system noise.

Intensity measurements can also be used to characterize underwater ambient noise fields. The energy density of an acoustic field is the sum of contributions from the active and reactive components. However the time-averaged acoustic intensity associated with the reactive part of the field is zero³. Therefore, measurements of both the energy density and intensity of an ambient noise field allow the active and reactive parts of the field to be resolved.

Hickling and Wei⁴ have previously demonstrated an underwater intensity array. In their system, four hydrophones were located at the vertices of a regular tetrahedron. The signals from the four hydrophones were processed to yield approximations to the pressure gradient at the center of the array along three orthogonal axes, thus giving the three components of the intensity vector. In SIRA, six hydrophones are used which allows pressure gradients to be determined directly from the difference signals of co-axial hydrophones.

3. Description of instrument

SIRA was developed under contract for DREA by Guigné International Ltd. (GIL), Paradise, Nfld., Canada. SIRA was designed to make intensity measurements over the frequency range 100 to 6000 Hz. To achieve this range, the mounting structure can be configured for two different hydrophone spacings, 8 cm or 19 cm. The 19 cm spacing is used to make measurements at frequencies down to 100 Hz while the 8 cm spacing allows measurements to be made up to 6000 Hz. Neither spacing can provide measurements over the entire frequency range as a result of the trade-off between errors in approximating the pressure gradient at high frequencies and susceptibility to noise at low frequencies, where the gradient is small.

The hydrophones used in SIRA are model 1042 transducers from International Transducer Corp., Santa Barbara, CA. They are 35 mm-diameter spheres and are omnidirectional to better than 0.5 dB below 25 kHz. The hydrophones have sensitivities of approximately $-200 \text{ dB}/\mu\text{Pa}$ in the band 1 kHz to 10 kHz. A photograph of the array with hydrophone spacing of 8 cm is shown in Fig. 1

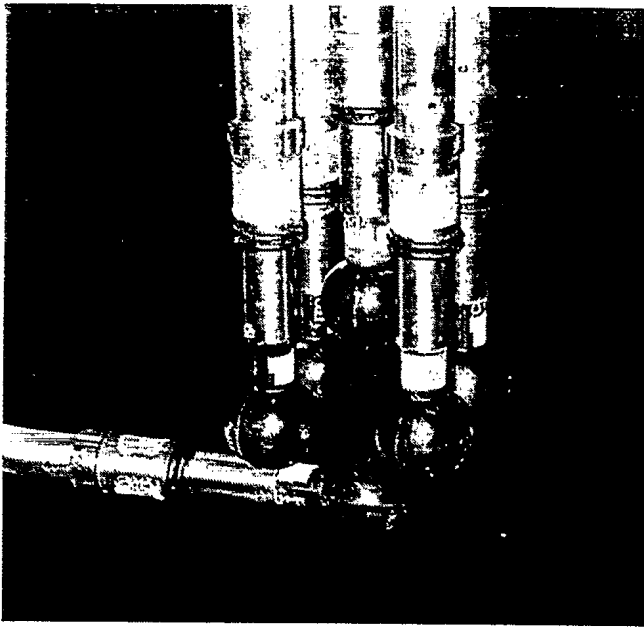


Fig. 1 Close-up of SIRA hydrophones and supporting structure. The hydrophone spacing is 8 cm.

The SIRA preamplifiers, custom-built by GIL, have built-in high and low pass filters with cutoff frequencies of 100 Hz and 20 kHz, respectively. The preamplifiers have a 12 dB fixed gain at the input stage with 60 dB of additional gain selectable in 12 dB increments. All preamplifiers had 60 dB gain for the measurements presented here. At 1 kHz, the pre-amplifier noise is less than $-165 \text{ dB/V/Hz}^{1/2}$ at all gain settings. Phase matching between the six preamplifiers is better than $\pm 0.3^\circ$ across the frequency band. The preamplifiers were paired to minimize the phase mismatch along each SIRA axis. Phase matching between pairs is better than $\pm 0.05^\circ$ across the frequency band. The inter-channel gain matching between all preamplifiers is better than $\pm 0.3 \text{ dB}$ and gain matching between axial pairs is better than $\pm 0.1 \text{ dB}$. Plots of the preamplifier phase and gain can be seen in Ref. 5.

The SIRA mechanical apparatus is made up of a tubular pressure vessel 20 cm in diameter by 63.5 cm long which contains the preamplifiers and other electronics. The pressure vessel is rated for a water depth of 300 m. The hydrophones are supported at the end of 1-m long stainless steel tubes which are attached to the bottom of the pressure vessel as shown in Fig. 2. The total mass of SIRA is approximately 60 Kg.

The spacing and orientation of the hydrophones must be precisely adjusted to minimize errors in the measured intensity. To facilitate hydrophone alignment, GIL developed a jig that allows the position of the hydrophones to be adjusted to within $\pm 1 \text{ mm}$ of the desired location. This corresponds to a positioning accuracy of $\pm 1.3\%$ for the 8 cm spacing and $\pm 0.5\%$ for the 19 cm spacing. The hydrophone alignment jig is shown in Fig. 3.

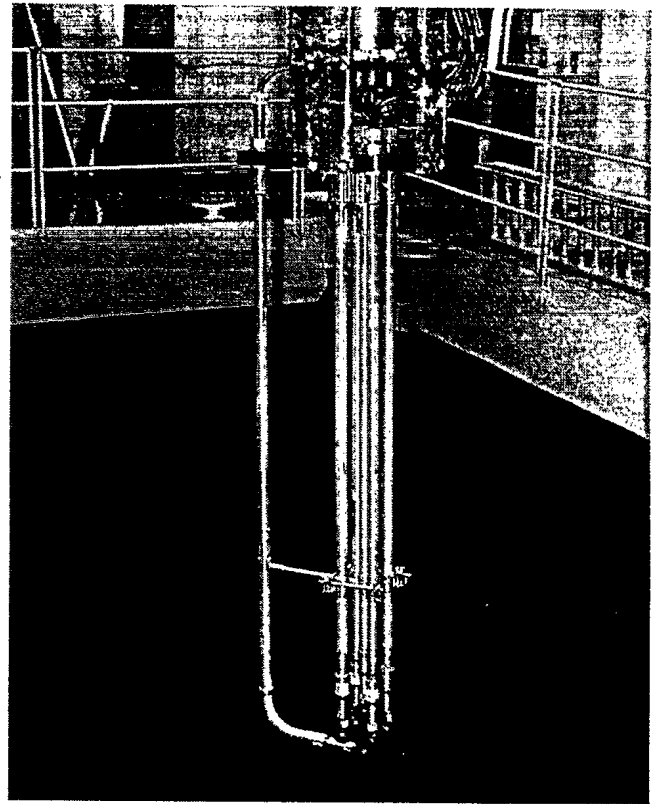


Fig. 2 Photograph of SIRA showing the 1 m-long tubular hydrophone supports attached to the bottom of the pressure vessel.

4. Intensity signal processing

The magnitude of the intensity component in direction \bar{x} is the time averaged product of the instantaneous acoustic pressure $p(t)$ and the particle velocity component $u_x(t)$,

$$I_x = \overline{p(t) \cdot u_x(t)} \quad (1)$$

SIRA uses pressure transducers to provide both pressure and particle velocity. This is referred to as the pressure-pressure method. The particle velocity is derived from the pressure gradient using the finite difference approximation,

$$u_x(t) = \frac{1}{\rho} \int_0^t \frac{p_{x2} - p_{x1}}{d} dt \quad (2)$$

where ρ is the water density and d is the distance between hydrophones x_1 and x_2 . Equation 2 yields an exact value for the particle velocity in the limit of vanishingly small kd . In practice, kd must be large enough to give a measurable difference signal. It is easily shown that the error in $u_x(t)$ as calculated with Eq. 2 is only 5% for $kd = 1$ and 17% for $kd = 2$. For the 8 cm spacing of the SIRA hydrophones, $kd = 1$ represents a frequency of 3 kHz and $kd = 2$ represents a frequency of 6 kHz. The benefits of increased signal to noise ratio justify the measurement of intensity at these relatively high kd values.

6. Intensity measurements

6.1 Dipole response functions

The performance of the intensity array can be evaluated by measuring the difference signal of hydrophone pairs for a narrowband acoustic wave as a function of array rotation angle. Ideally, when a pair of hydrophones is aligned with their axis perpendicular to the direction to the source, the received signals should cancel. In this orientation, any difference signal is due to imbalance in gain and phase response, scatter from the array components and the presence of system electronic noise and acoustical ambient noise. For $kd \ll 1$, and assuming a plane acoustic wave, the measured difference signals can be compared to an ideal dipole. An example is shown in Fig. 6 where measured data are displayed as dots and the curves are those of an ideal dipole given by $\cos(\theta)$ for the x axis and $\sin(\theta)$ for the y axis.

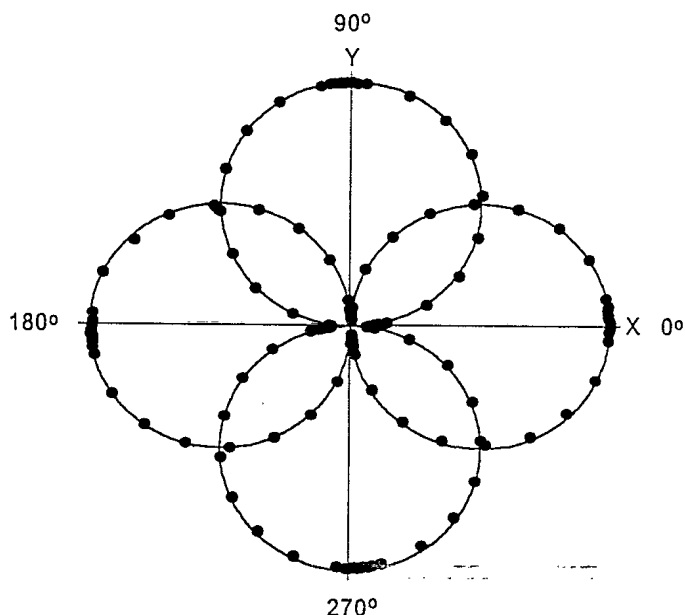


Fig. 6 Measured difference signals (points) and ideal dipole response (curves) for $d = 19$ cm and $f = 500$ Hz, plotted on a linear scale.

The measurements shown in Fig. 6 were made at a frequency of 500 Hz with a hydrophone spacing of 19 cm ($kd = 0.4$). The data points are based on the coherent average of 10 pulses, each of 10 ms duration. Data are normalized by the maximum value at the dipole lobes. The signal to noise ratio was approximately 35 dB during the measurements. The agreement between the measurements and ideal dipole indicates good performance for the horizontal SIRA channels. The symmetry of the dipole plots shows that the inter-channel phase matching is good. This is consistent with the fact that the best phase matching occurs at 500 Hz with an error of approximately 0.2° .

For the data shown in Fig. 6, the average value of the x and y nulls is 4.9% of the lobe maxima. If the data were expressed as intensity, the mean of the nulls would be -26 dB with respect to the lobe maxima. Measurements of the dipole pattern were obtained for frequencies from 500 Hz to 4000 Hz. The deepest set of nulls was obtained at 4000 Hz with a value of -32.5 dB. The presence of unavoidable ambient noise contributes to the residual difference signal at the nulls. Measurements made under quieter conditions and with greater angular resolution near the nulls could reveal that the SIRA nulls are deeper than presented here. Also, it is possible to correct for the measured channel phase and gain imbalances which could result in even better performance.

6.2 Direction to signal source

Processing the data of Fig. 6 to yield the x and y intensity vector components allows the direction to the source to be calculated via Eq. 4. A comparison of the calculated direction to the source and the measured array orientation angle is shown in Fig. 7. The standard deviation of the difference between measured and calculated angles is 1.4° . Although the width of the array is only 6% of a wavelength at 500 Hz, intensity processing allowed the direction to the source to be determined with an accuracy of 1.4° . Using conventional beamforming methods, an array would have to be several wavelengths in size to measure the direction to the source with the same accuracy.

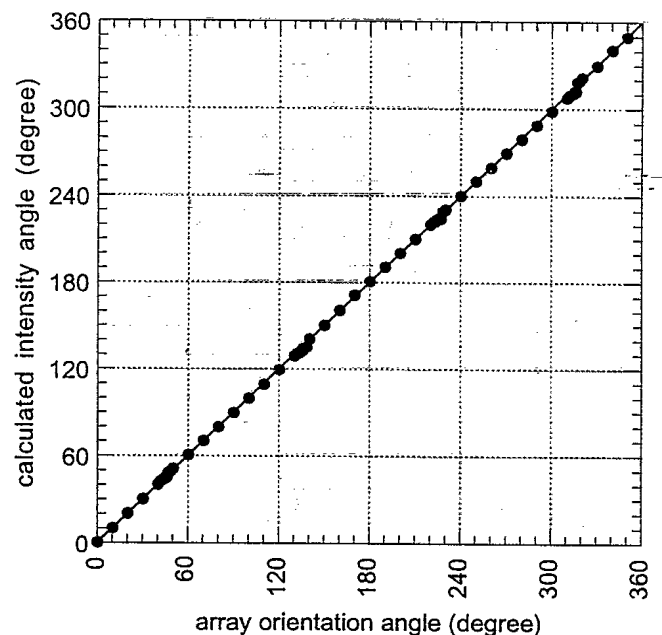


Fig. 7 Direction to acoustic source calculated from intensity vector components using Eq. 4 for $f = 500$ Hz and $d = 19$ cm.

7. Effect of ambient noise on intensity

If system electronic noise, turbulent flow noise and scattering noise can be kept well below the level of ambient noise, then the ambient noise will be the main contributor to error in the intensity measurements. One of the effects of noise on the calculated intensity is to increase the variance of intensity values derived from a series of pulses. We measured the effect of ambient noise on the standard deviation σ_I of measured intensity by recording series of 10 ms-long pulses at different projector source levels. The ambient noise level was obtained from the 10 ms periods preceding the arrival of each pulse and used to calculate the signal to noise ratio, SNR . The standard deviations of intensity obtained from groups of 8 pulses, normalized by the mean \bar{I} are shown in Fig. 8 as a function of SNR . The data were obtained using both x and y horizontal hydrophone pairs at 1 kHz. The data show the expected decrease of σ_I/\bar{I} as SNR increases. A functional relationship between the data points is suggested by a least-squares power law fit which appears on Fig. 8 as a straight line. A theoretical model of the relationship between σ_I/\bar{I} and SNR would allow the accuracy of intensity measurements to be predicted given the measurement conditions.

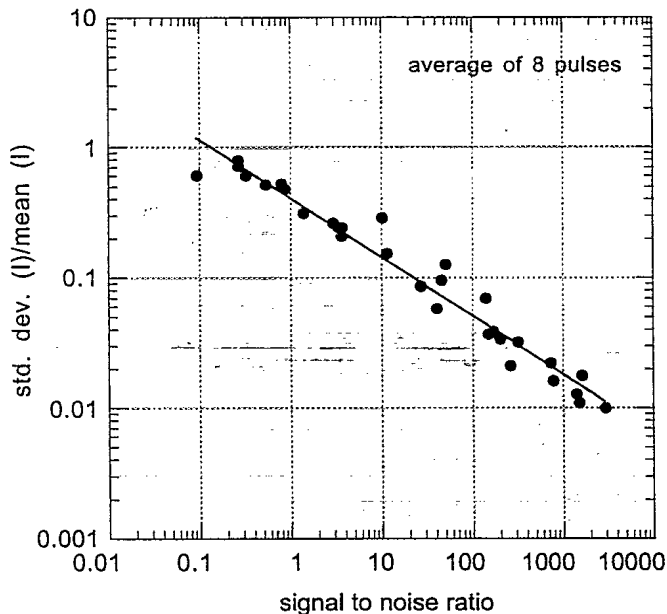


Fig. 8 Standard deviation of groups of 8 pulses, normalized by the mean \bar{I} , as a function of SNR .

8. Characteristics of ambient noise

The ability of the intensity array to reject ambient noise is a function of the coherence of the noise at the frequency of interest⁷. Any time-averaged phase difference between noise signals, which is represented by the imaginary part of the cross-spectrum, contributes to the mea-

sured intensity. The normalized cross-spectrum $S_{1,2}(\omega)$ is defined by

$$S_{1,2}^2(\omega) = \frac{S_1(\omega)S_2^*(\omega)}{|S_1(\omega)||S_2(\omega)|} \quad (5)$$

$S_{1,2}(\omega)$ for ambient noise at the DREA barge is shown in Figs. 9 and 10 for the z (vertical) and y (horizontal) hydrophone pairs. During the measurements the wind speed was 20 km/hr with wave height 0.5 m.

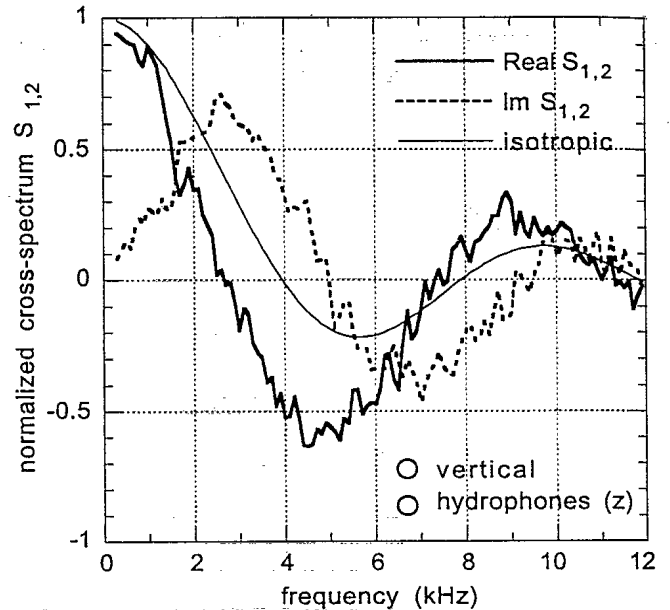


Fig. 9 Cross-spectrum $S_{1,2}(\omega)$ of ambient noise for vertical (z) hydrophone signals.

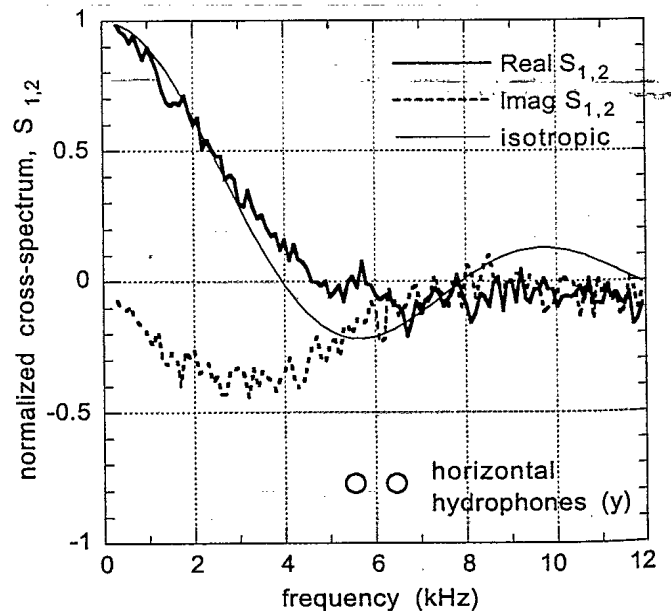


Fig. 10 Cross-spectrum of ambient noise for horizontal (y) hydrophone signals.

The cross-spectra shown in Figs. 9 and 10 are compared to the theoretical curve that would be expected for isotropic ambient noise where the real part of $S_{1,2}(\omega)$ is given by $\sin(kd)/kd$ and the imaginary part is zero¹. $S_{1,2}(\omega)$ for the vertical pair is substantially different from the isotropic case and has a significant imaginary component. The real part is similar to that caused by a surface distribution of dipole noise sources as described in Ref. 8. The vertical anisotropy of the noise is attributed to the effect of the highly absorbing mud bottom at the barge location.

The ambient noise in the horizontal plane is much more isotropic than it is in the vertical sense as shown by the cross-spectrum in Fig. 10. In the frequency range where SIRA operates, 100 to 6000 Hz, the imaginary component of $S_{1,2}(\omega)$ for the horizontal plane is approximately half that for the vertical. Since the imaginary part of $S_{1,2}(\omega)$ is equivalent to intensity normalized by mean signal power, these results indicate that ambient noise would contribute significantly more error to intensity measured with the vertical pair as it would with a horizontal pair.

9. Conclusion

SIRA is an experimental intensity array composed of three hydrophone pairs aligned along orthogonal axes. Each pair provides one of the components of the three dimensional intensity vector in the frequency range 100 to 6000 Hz. SIRA was developed under contract for DREA by Guigné International Ltd. Preliminary measurements made with SIRA at the DREA calibration barge facility were presented.

Comparison of difference signals measured with the horizontal hydrophone pairs to the angular sensitivity pattern of an ideal dipole indicate good inter-channel gain and phase balance. By rotating the array in the presence of an acoustical source, the direction to the source was derived from the x and y intensity components and shown to be accurate to 1.4°. This highlights one of the advantages of intensity arrays which is that accurate directional localization of a source can be made with an array that is much smaller than a wavelength.

Ambient noise degrades intensity measurements by increasing the intensity variance. The relationship between signal to noise ratio and the variance of intensity measurements was demonstrated. However a theoretical model of the effect of noise on calculated intensity magnitude and phase is required in order to predict the statistics of intensity measurements for given conditions.

Finally, the array was used to analyze the ambient noise field in the vertical and horizontal directions by calculating the cross-spectra of signals from hydrophone pairs. The results show that the ambient noise was much more isotropic in the horizontal plane than it was in the vertical.

In the results presented here, array signals were not corrected for known inter-channel phase and sensitivity imbalances. We intend to implement these corrections in future versions of the SIRA signal processing software.

10. Acknowledgements

The authors gratefully acknowledge the technical support of Roger Arsenault, Paul Shouldice, Dave Doucette, Dave Lewis and Ron Cunningham.

11. Reference

1. Urick, R. J., *Ambient Noise in the Sea*, Chap. 6, Peninsula Publishing, Los Altos (1986).
2. Lo, E. Y. and M. C. Junger, "Signal-to-noise enhancement by underwater intensity measurements", *J. Acoust. Soc. Am.* 82(4) 1450-1454 (1987).
3. Shchurov, V. A., "Coherent and diffusive fields of underwater acoustic ambient noise", *J. Acoust. Soc. Am.* 90(2) 991-1001 (1991).
4. Hickling, R. and W. Wei, "Finding the direction of a sound source using a vector sound intensity probe", *J. Acoust. Soc. Am.* 94(4) 2408-2412 (1993).
5. Hines, P. C. and D. Hutt, "SIREM: An instrument to evaluate superdirective and intensity receiver arrays", *Proc. Oceans'99* (this volume).
6. Fahy, F. J., *Sound Intensity*, Elsevier Applied Science, London (1989).
7. Franklin, J. B., "Intensity measurements and optimum beam forming using a crossed dipoles array", *Defence Research Establishment Atlantic, DREA CR/97/443* (1997).
8. Cron, B. F., B. C. Hassell and F. J. Keltonic, "Comparison of theoretical and experimental values of spatial correlation", *J. Acoust. Soc. Am.* 37(3) 523-529 (1965).

#513113